E-Journal of Advanced Maintenance Vol.7-1(2015) 50-58
Japan Society of Maintenology

Correction of Over and Under Exposure Images Using Multiple Lighting System

Jonghoon IM[1*], Hiromitsu FUJII[1], Atsushi YAMASHITA[1], and Hajime ASAMA[1]

[1] *The University of Tokyo, 7-3-1 Hongo, Bunkyo-ku, Tokyo 113-8656, Japan*

ABSTRACT

When images are acquired in bright condition, it can cause a loss of highlight details (over exposure) in bright area and a loss of shadow details (under exposure) in dark area. Over and under exposure causes a big problem when people investigate dangerous place like Fukushima nuclear power plant through the camera attached remote control robot. In this paper, we propose a method to correct the over and under exposure image to solve the problem. The image processing consists of four steps. Firstly, multiple images are acquired by alternately turning on and off each illumination which set in different positions. Then the image obtained first is defined as input image 1, the image obtained second is defined as input image 2 and the image obtained *N*-th is defined as input image *N*. Secondly, luminance of the images is corrected. Thirdly, over and under exposure regions in the image are extracted from the input image 1. Finally, the over and under exposure regions in the input image 1 are compensated by other images. The results show that the over and under exposure regions in the input image are recovered by our proposed method.

KEYWORDS

Image processing, Multi-exposure images fusion, Image correction, Over and under exposure, Multiple lighting system

ARTICLE INFORMATION

Article history:
Received 5 November 2014
Accepted 26 February 2015

1. Introduction

It is necessary to use remote control robots when people investigate dangerous place where they cannot enter. Especially, it is necessary to use some lightings which are attached to the robot in dark area without external lighting in order to obtain the information of surrounding as shown in Fig. 1. In this case, the problem is that a portion of the image is unclear because of over and under exposure. In order to solve this problem, Multi-Exposure Fusion (MEF) techniques[1][2][3][4] and High Dynamic Range (HDR) imaging techniques[5][6][7] have been proposed. These techniques are obtaining one image by combining a plurality of images with different exposure level. In the HDR imaging, a high dynamic range image is compressed into a low dynamic range image using tone mapping

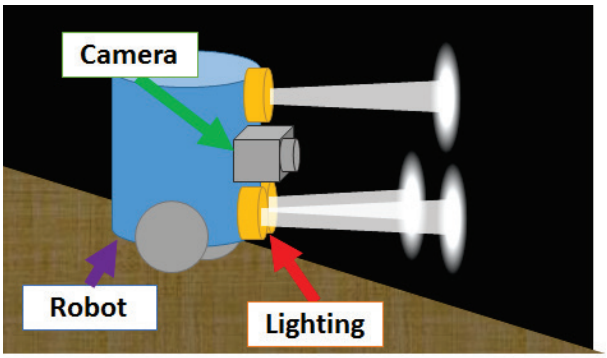

Fig. 1. Investigation using remote controlled robot.

*Corresponding author, E-mail: im@robot.t.u-tokyo.ac.jp

methods[8][9] for viewing on ordinary displays. And it needs the calibration of the camera response function (CRF) which is required in HDR imaging if the CRF is not linear. However, MEF does not need these process, and has low computational complexity. So, we propose a method of correction over and under exposure which is based on MEF.

In the general HDR imaging, the magnitude of the luminance values between the pixels is preserved before and after tone mapping. For this reason, the available dynamic range in each region is limited in the environment that has large contrast. And it is difficult to store all the texture information to the HDR image because of the constraint condition. And in the previous HDR imaging and MEF methods use a beam splitter[10][11] or adjust camera's shutter speed[12][13][14] to acquire multiple images having different exposure value. In the former case, it is need to specific and expensive device. And it is difficult to acquire multiple images whose exposure values are appropriate by adjusting camera's shutter speed in the environment that has large contrast in the latter case. To solve these problem, we use multiple lightings to acquire multiple images whose locations of the over and under exposure areas are different from each other.

In this paper, we propose a method to correct the over and under exposure region in the image using multiple lighting system. We assume the situation that operator investigates in a dark environment using a remote control robot like Fig. 1. Multiple lightings, such as the headlights of the car are attached to the front of the robot, and each lighting can be turned on and off by the operator.

The rest of the paper is organized as follows. Section 2 describes proposed method, and Section 3 depicts experiment and the result. Finally, Section 4 concludes the paper.

2. Proposed method

Our method consists of image acquisition, luminance correction, extraction of over and under exposure areas and compensation of over and under exposure areas. The proposed method is shown in Fig. 2. Each step is described in detail and three prepared sample images are used for explaining the process of our proposed method.

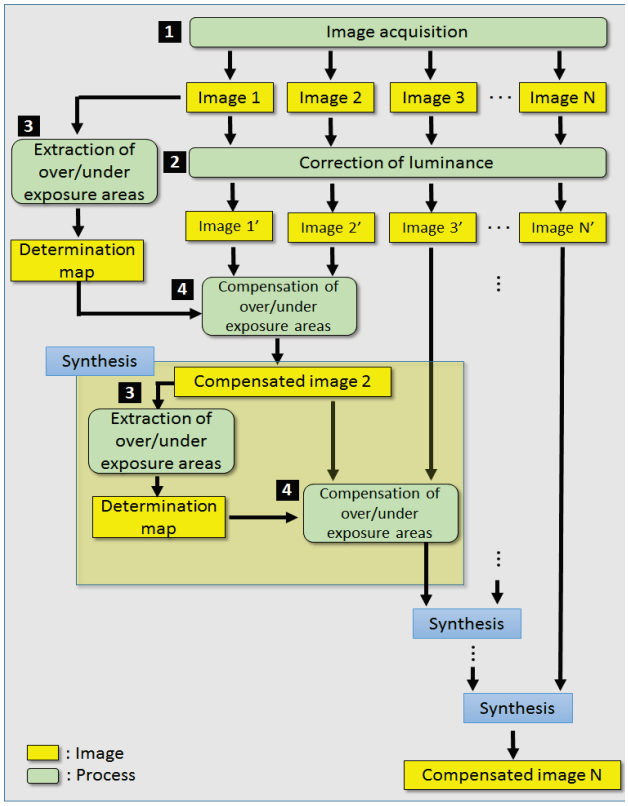

Fig. 2. The schematic view of our proposed method for correction of over/under exposure.

(a) (b) (c) (d)

Fig. 3 Background image and input images: (a) Background image, (b) Input image 1 I_0^1, (c) Input image 2 I_0^2 and (d) Input image 3 I_0^3.

2.1. Image acquisition

In this process, multiple photographs that over and under exposure appeared in different location are captured by changing lighting condition at the same background (Fig. 3(a)). In this research, multiple images are acquired by alternately turning on and off each illumination which set in different positions. The image obtained first is defined as input image 1 $\boldsymbol{I}_0^1$, the image obtained second is defined as input image 2 $\boldsymbol{I}_0^2$ and the image obtained N-th is defined as input image N $\boldsymbol{I}_0^N$. Fig. 3 shows sample images which were taken with a real camera to explain the process of our proposed method. The subjects in the images are a $1.29\text{m} \times 0.73\text{m}$ printed picture which describes inside of Fukushima nuclear power plant. The over exposure is appeared in the lower left and the under exposure is appeared in the upper right in the input image 1 (Fig. 3(b)). On the other hand, the over exposure is appeared in the lower right and the under exposure is appeared in the left in the input image 2 (Fig. 3(c)). In the input image 3 (Fig. 3(d)), the over exposure is appeared in the upper middle and the under exposure is appeared in the lower left and right.

2.2. Luminance correction

The brightness distribution of the acquired images are changed by the illumination. It can be confirmed by comparing Fig. 3 (b), (c) and (d) that is acquired by changing light condition. In order to obtain a clear image, it is necessary to correct the brightness distribution of the acquired images. In this step, firstly we find the center of irradiated area, secondly correct the brightness of each pixel by considering distance from the center of the irradiated area.

In order to find the center of irradiated area, firstly the over exposure areas that are caused by lightings are extracted. One threshold value τ_C which is set in advance is used for the extraction as shown equation (1).

$$\boldsymbol{C}^n(i,j) = \begin{cases} 1 & \text{if } \boldsymbol{I}_0^n(i,j) > \tau_C \\ 0 & \text{otherwise} \end{cases}, \qquad (n = 1,2,\cdots N) \tag{1}$$

(a) (b) (c)

Fig. 4. Irradiated area images: (a) Irradiated area image $\boldsymbol{C}^1$, (b) Irradiated area image $\boldsymbol{C}^2$ and (c) Irradiated area image $\boldsymbol{C}^3$. The over exposure areas are displayed in green and non-over exposure areas are displayed in black. The position of center of irradiated area is displayed in red circle.

where n is the number of input image, $\boldsymbol{I}_0(i, j)$ is the pixel value of an original input image. $\boldsymbol{I}_0^n(i, j)$ is the pixel value of the original input image n coordinates (i, j).The pixel value describes how bright that pixel is. $\boldsymbol{C}^n$ is the obtained image as a result of luminance correction process, and the image is defined as an irradiated area image $\boldsymbol{C}^n$. Color images are converted into grayscale image before process. If the pixel value of the image n coordinates (i, j) is over τ_C which is set in advance by considering environment and lighting condition, it is determined over exposure area and the pixel value is converted to 1. Otherwise it is determined non-over exposure area and the pixel value is converted to 0. As a result, the irradiated area $\boldsymbol{C}^n$ is acquired (Fig. 4(a)), we convert grayscale image to color image in order to make it easier to view the extracted area. The over exposure areas are displayed in green and non-over exposure areas are displayed in black in the Fig. 4(a). Next, the center of the irradiated area in the over exposure areas is searched by calculating the average value of i and j coordinates of the green pixels as shown equation (2). M is the number of green pixels in the irradiated area image $\boldsymbol{C}^n$. Acquired position of the center of the irradiated area set to (X_c, Y_c). The position is displayed in red circle in the Fig. 4(a). The same procedure is performed in other input images (Fig. 4(b), (c)).

$$Xc = \frac{\sum_{x \in \{i \mid \boldsymbol{C}(i,j)=1\}} x}{M}, \quad Yc = \frac{\sum_{y \in \{j \mid \boldsymbol{C}(i,j)=1\}} y}{M}, \tag{2}$$

Then, we correct the luminance of the images using distance between the center of the irradiated area and each pixel. In Fig. 3(b), (c) and (d), around the center of the irradiated area is the brightest. And the luminance become gradually darker when the distance between the center of the irradiated area and each pixel become longer. In order to correct the luminance of the images, equations (3), (4) and (5) are used.

$$\boldsymbol{L}'(i, j) = f(\boldsymbol{L}(i, j)), \tag{3}$$

$$f(\boldsymbol{L}(i, j)) = \alpha \cdot \boldsymbol{L}(i, j) \cdot r^2, \tag{4}$$

$$r = \sqrt{(i - X_c)^2 + (j - Y_c)^2}, \tag{5}$$

where $f(\boldsymbol{L}(i, j))$ is a luminance correction function, $\boldsymbol{L}(i, j)$ is a luminance value at the coordinates (i, j) before luminance correction and $\boldsymbol{L}'(i, j)$ is a luminance value at the coordinates (i, j) after luminance correction. α is correction factor which is set in advance by considering environment condition and it keep the luminance value from becoming very large. r is the distance between the center of the irradiated area and each pixel. X_c and Y_c are the position of the center of the irradiated area. We use equation (4) as the luminance correction function in this time. Equation (4) is an approximate equation for correcting the luminance of the input image using the principle that the brightness is inversely proportional to the square of the distance from the center of irradiated areas to each pixel. The brightness is equalized by multiplying the brightness of each pixel from input image and the square of the distance. The luminance correction value in equation (4) is determined depending on the distance from the center of the over exposure area, regardless of the shape of the object. As a result of the luminance correction, luminance corrected image $\boldsymbol{I}_p$ is acquired. $\boldsymbol{I}_p^n$ is luminance corrected image of input image $\boldsymbol{I}_0^n$, Fig. 5(a), (b) and (c) shows $\boldsymbol{I}_p^1$, $\boldsymbol{I}_p^2$ and $\boldsymbol{I}_p^3$.

2.3. Extraction of over and under exposure areas

This process extracts the over and under exposure areas in an image in order to get rid of these areas. Two threshold values τ_H and τ_L which are set in advance are used for the extraction as shown equation (6).

$$\boldsymbol{D}(i, j) = \begin{cases} 1 & \text{if } \tau_L < \boldsymbol{I}(i, j) < \tau_H \\ 0 & \text{otherwise} \end{cases}, \tag{6}$$

(a) (b) (c) (d)

Fig. 5 Luminance corrected images and determination map: (a) Luminance corrected image I_p^1, (b) Luminance corrected image I_p^2, (c) Luminance corrected image I_p^3 and (d) determination map D^1.

where $\boldsymbol{I}(i, j)$ is a pixel value of the input image coordinates (i, j). $\boldsymbol{D}$ is the reference matrix for determining over and under exposure areas, which is obtained as a result of the extraction process of over and under exposure. This reference matrix is defined as a determination map. If the pixel value of the input image coordinates (i, j) is over τ_H which is set in advance, it is determined over exposure areas and the pixel value is converted to 0. If the pixel value of the input image coordinates (i, j) is under τ_L which is set in advance, it is determined under exposure areas and the pixel values is converted to 0. Otherwise, if the pixel value of the image coordinates (i, j) is included between τ_H and τ_L, it is determined non-over and under exposure areas and the pixel value is converted to 1. As a result, the determination map $\boldsymbol{D}$ is acquired. Fig. 5(d) shows determination map of the input image 1 (Fig. 3(b)). The over and under exposure areas are displayed in black and non-over and under exposure areas are displayed in white in the Fig. 5(d).

2.4. Compensation of over and under exposure areas

In this step, the over and under exposure areas of the image 1 are compensated by other images. The determination map $\boldsymbol{D}$ which is obtained in Section 2.3 is used. The rule of the synthesis is shown in equations (7) and (8).

$$\boldsymbol{I}_f^n(i,j) = \begin{cases} \boldsymbol{I}_f^{n-1}(i,j) & D^{n-1}(i,j)=1 \\ \boldsymbol{I}_p^n(i,j) & D^{n-1}(i,j)=0 \end{cases}, \quad (n \geq 2) \tag{7}$$

$$\boldsymbol{I}_f^1(i,j) = \boldsymbol{I}_p^1(i,j) \ ,$$

$$\frac{\sum \left| \boldsymbol{I}_f^n(i,j) - \boldsymbol{I}_f^{n-1}(i,j) \right|}{\sum \boldsymbol{I}_f^n(i,j)} \leq \beta \tag{8}$$

where $\boldsymbol{D}^n$ is a determination map of luminance corrected image n $\boldsymbol{I}_p^n$ except $\boldsymbol{D}^1$. $\boldsymbol{D}^1$ is a determination map of input image 1 $\boldsymbol{I}_0^n$. $\boldsymbol{I}_f$ is an output image whose over and under exposure areas were compensated. $\boldsymbol{I}_f{}^n$ is the output image when n images are used. The areas where $\boldsymbol{D}^{n-1}$ (i, j)=1 in the determination map are compensated by the image $\boldsymbol{I}_f{}^{n-1}$, and the areas where $\boldsymbol{D}^{n-1}$ (i, j)=0 in the determination map are compensated by the image $\boldsymbol{I}_p^n$. As a result of this process, compensated image $\boldsymbol{I}_f{}^n$ is obtained. The process will proceed until n=N. However, it is not efficient to use all of the images for the compensation because the computational time becomes longer. In order to reduce the computational time, we set a termination condition of the compensation algorithm. If the rate of change of pixel value between $\boldsymbol{I}_f{}^n$ and $\boldsymbol{I}_f{}^{n-1}$ is less than β which was decided on the basis of previous experimental result as shown in equation (8), the process is over. For example, when N=3, the areas where $\boldsymbol{D}^1$ (i, j)=1, which are shown as white in Fig. 5(d), are compensated by the image $\boldsymbol{I}_p^1$ (Fig. 5(a)). The areas where $\boldsymbol{D}^1$ (i, j)=0, which are shown as black in Fig. 5(d), are compensated by the image $\boldsymbol{I}_p^2$ (Fig. 5(b)). As the result of the compensation, the output image 2 $\boldsymbol{I}_f{}^2$ (Fig. 6(a)) is obtained. Next, output image 2 $\boldsymbol{I}_f{}^2$ is compensated by the image $\boldsymbol{I}_p^3$(Fig. 5(c)) and determination map $\boldsymbol{D}^2$(Fig. 6(b)) in the same way. As the result of the compensation, the output image 3 $\boldsymbol{I}_f{}^3$ (Fig. 6(c)) is obtained.

(a) Output image2 I_f^2 (b) Determination map D^2 (c) Output image3 I_f^3

Fig. 6. Output images when N=3.

Table 1. Photographing conditions.

Camera	NIKON D200
Definition	640 ×480
ISO	2,500
F-number	*f*/8
Shutter speed	1/40sec
Focal length	24mm
Luminance of lighting	1,000lm

3. Experiment

3.1. Experiment environment

In the experiment, we used four lightings in order to acquire four images that over and under exposure appeared in different location. For the experiment, we prepared two signs in advance (Fig. 7(a)). 'DANGER Radiation risk' letters were written on the left side sign, and 'DO NOT ENTER, STAFF ONLY' letters were written on the right side sign. Fig. 7(b) shows the distance between the signs and the camera, and Fig. 7(c) shows the distance between the camera and the lightings. The height of the camera was 8.50×10^{-1}m from the floor, and the distance between the signs and camera was 2.00m as shown in Fig. 7(b). The lighting 1 was located in 2.00×10^{-1}m under 3.00×10^{-1}m left side of the camera, the lighting 2 was located in 2.00×10^{-1}m under 3.00×10^{-1}m right side of the camera. The lighting 3 was located in 2.00×10^{-1}m upper of the camera and the lighting 4 was located in 2.00×10^{-1}m under of the camera as shown in Fig. 7(c). All of the photographing conditions were fixed except the distance between the camera and the lightings during the image acquisition process. The photographing conditions are depicted in Table 1. Finally, four images are acquired by alternately turning on and off each lighting which set in different positions.

3.2. Experiment results

All experiments are simulated on an Intel Core^{TM} i5-2520M CPU 2.50 GHz PC with 8 GB RAM. The computing time of the proposed method is about 0.19 seconds by single thread coding in C++. Fig. 8 shows the experiment results. Fig. 8(a), (b), (c) and (d) shows the input image 1, 2, 3 and 4. Figures 8(e), (f) and (g) described the output image 2, 3 and 4 which were combined by our proposed method. In this experiment, we set the τ_H=200, τ_L=5, τ_C=200, α=1.3×10^{-4} and β=0.1.

In the input image 1, the over exposure appeared on the left side sign and the under exposure appeared on the right side of the image. In consequence, the letters which were written on the left sign became unclear. Also the right side of the image cannot identify because of the under exposure. On the other hand, in the input image 2, the over exposure appeared on the right side sign and the under exposure appeared on the left side of the image. As a result, the letters which were written on the right

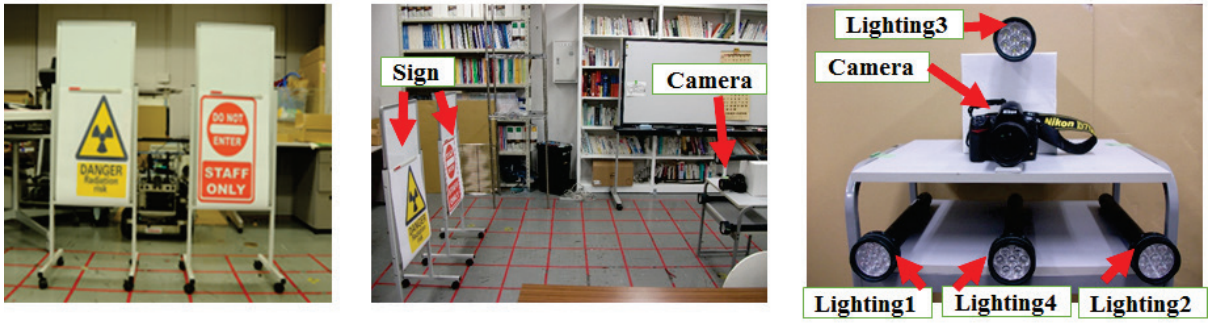

(a) Two signs (b) Distance between signs and camera (c) Distance between camera and lightings

Fig. 7. Experiment environment.

(a) Input image 1 I_0^1 (b) Input image 2 I_0^2 (c) Input image 3 I_0^3

(d) Input image 4 I_0^3 (e) Output image 2 I_f^2 (f) Output image 3 I_f^3

(g) Output image 4 I_f^4 (h) Contrast compensation (i) HDR imaging[7]

Fig. 8. Experiment results.

sign became unclear. The left side of the image cannot identify because of the under exposure. In the input image 3 and 4, the over exposure appeared on the center of the image and the under exposure appeared on the edge of the image. As a result of applying the proposed compensation algorithm to the input image 1, the over exposed areas in the input image1 became clear, and 'DANGER Radiation risk' letters became visible. Also, the under exposed areas in the input image 1 were compensated and the areas became clear. The rate of the pixel change of output image 2, 3 and 4 were 0.59, 0.07 and 0.01. The process terminated when the output image 3 was synthesized. The process time of each case

were 0.12, 0.19 and 0.26 seconds. As the results of the termination condition, the computation time reduced by 0.07 seconds.

Next, we compared the result of the proposed method (Fig. 8(f)), contrast compensation (Fig. 8(h)) and HDR imaging (Fig. 8(i)) [7]. Fig.9 shows hue histogram of original image, the result of contrast compensation, the result of HDR imaging and the result of our proposed method. X-axis of the histogram represents a hue value [0,180] and Y-axis represents a frequency of each hue value. The hue value is more evenly distributed in the result of the proposed method than the original image, the result of HDR imaging and contrast compensation. In order to view whole scene in the environment that has large contrast, it is need to the hue values which are uniformly distributed. The experimental result shows that our proposed method is better than the previous contrast compensation and HDR imaging.

4. Conclusion

In this paper, we proposed the method of correction the over and under exposure images using multiple lighting system. We assume the situation that operator investigates in a dark environment using a remote control robot, and in this time, multiple lightings, such as the headlights of the car are attached to the front of the robot, and each lighting can be turned on and off by the operator. And we build experimental environment that we assumed. Next, multiple images were acquired using multiple lighting system. Finally, the over and under exposure areas were compensated by the proposed method. The experimental results showed the effectiveness of our proposed method.

In this research, we fixed the threshold value τ_c, and correction factor α. And we decide the value appropriately by considering experiment environment. However, the appropriate value is changed by the environment and lighting condition. So we are considering to decide the value automatically for future work. And we plan to apply our method to real situation such as Fukushima nuclear power plant. And it is necessary to control brightness of the light or adjust the angle of the light not only ON/OFF of the light in order to acquire more images in which the exposure values are different.

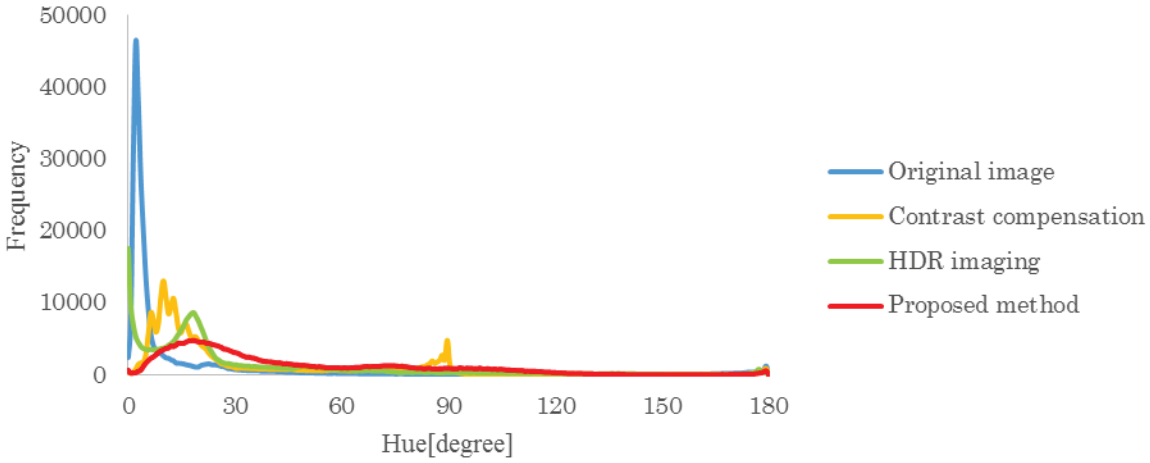

Fig. 9. Hue histogram of original image, the result of HDR imaging, the result of contrast compensation and the result of our proposed method.

Acknowledgement

This research was supported by the Agency for Natural Resources and Energy and International Research Institute for Nuclear Decommissioning, Japan, Fiscal Year 2013.

References

[1] T. Mertens, J. Kautz and F. Van Reeth: "Exposure Fusion: A Simple and Practical Alternative to High Dynamic Range Photography", *Computer Graph. Forum*, Vol. 28, No. 1, pp. 161-171(2009).
[2] R. Shen, I. Cheng and A. Basu: "QoE-Based Multi-Exposure Fusion in Hierarchical Multivariate Gaussian CRF", *IEEE Transactions on Image Processing*, Vol. 22, No. 6, pp. 2469-2478(2013).
[3] A. Agrawal, R. Raskar, S. Nayar and Y. Li: "Removing Photography Artifacts Using Gradient Projection and Flash-Exposure Sampling", *Proceedings of ACM SIGGRAPH 2005,* Vol. 24, No. 3, pp. 828-835(2005).
[4] J. Kong, R. Wang, Y. Lu, X. Feng and J. Zhang: "A Novel Fusion Approach of Multi-exposure Image", *Proceedings of International Conference on "Computer as a Tool" 2007 EUROCON*, pp. 163-169(2007).
[5] S. Mann and R. W. Picard: "On being 'Undigital' with Digital Cameras : Extending Dynamic Range by Combining Differently Exposed Pictures", *Proceedings of the 48th Annual Conference of the Imaging Science and Technology*, pp. 442-448(1995).
[6] K. Agusanto, L. Li, C. Zhu and S. W. Ng: "Photo Realistic Rendering for Augmented Reality Using Environment Illumination", *Proceedings of the Second IEEE and ACM International Symposium on Mixed and Augmented Reality*, pp. 208-216(2003).
[7] P. Debevec and J. Malik: "Recovering High Dynamic Range Radiance Maps from Photographs", *Proceedings of ACM SIGGRAPH 1997*, pp. 369-378(1997).
[8] E. Reinhard, M. Stark, P. Shirley and J. Ferwerda: "Photographic Tone Reproduction for Digital Images", *Proceedings of ACM SIGGRAPH 2002*, pp. 267-276(2002).
[9] J. Kuang, G. M. Johnson and M. D. Fairchild: "ICAM06: A Refined Image Appearance Model for HDR Image Rendering", *Journal of Visual Communication and Image Representation*, Vol. 18, No. 5, pp. 406-414(2007).
[10] M. D. Tocci, C. Kiser, N. Tocci and P. Sen: "A Versatile HDR Video Production System", *ACM Transactions on Graphics*, Vol. 30, No. 4, pp. 41-50(2011).
[11] M. Aggarwal and N. Ahuja: "Split Aperture Imaging for High Dynamic Range", *Proceedings of IEEE International Conference on Computer Vision 2001*, pp. 10-17(2001).
[12] D. C. H. Schleicher and B. G. Zagar: "High Dynamic Range Imaging by Varying Exposure Time, Gain and Aperture of a Video Camera", *Proceedings of IEEE Instrumentation and Measurement Technology Conference 2010,* pp. 486-491(2010).
[13] Y. Piao and W. Xu: "Method of Auto Multi-Exposure for High Dynamic Range Imaging", *Proceedings of International Conference on Computer, Mechatromics, Control and Electronic Engineering 2010,* Vol. 6, pp. 93-97(2010).
[14] N. Barakat and T. E. Darcie: "Minimal Capture Sets for Multi-Exposure Enhanced-Dynamic-Range Image", *Proceedings of IEEE International Symposium on Signal Processing and Information Technology 2006*, pp. 524-529(2006).